

This discussion paper is/has been under review for the journal Atmospheric Chemistry and Physics (ACP). Please refer to the corresponding final paper in ACP if available.

Technical Note

J. Pavlovic and
P. K. Hopke

Technical Note: Detection and identification of radical species formed from α -pinene/ozone reaction using DMPO spin trap

J. Pavlovic and P. K. Hopke

Center for Air Resources Engineering and Science, Clarkson University, Potsdam, NY 13699-5708, USA

Received: 2 September 2009 – Accepted: 21 October 2009 – Published: 9 November 2009

Correspondence to: P. K. Hopke (hopkek@clarkson.edu)

Published by Copernicus Publications on behalf of the European Geosciences Union.

Title Page

Abstract

Introduction

Conclusions

References

Tables

Figures

⏪

⏩

◀

▶

Back

Close

Full Screen / Esc

Printer-friendly Version

Interactive Discussion



Abstract

The reactions of ozone with monoterpenes proceed via the formation of multiple oxygen- and carbon-centered free radical species. These radical species are highly reactive and thus, have generally not been measurable. A method for their detection and characterization is needed to preserve these radicals for a sufficiently long time to permit analyzes to be performed. Radical-addition reactions, also called spin trapping techniques, allow the detection of short-lived radicals. This approach has been applied to products from the α -pinene/ozone reaction. Secondary organic aerosol (SOA) from a reaction chamber was collected on quartz fiber filters and extracted with a solution of 5,5-dimethyl-1-pyrroline-N-oxide (DMPO) (spin trap) followed by analysis with ion-trap tandem mass spectrometry (MS^N) using electrospray ionization (ESI) in the positive scan mode. The DMPO adducts with radical species appear as positive ions $[DMPO-R+H]^+$, $[DMPO-OR+H]^+$ and $[DMPO-O-OR+H]^+$ in full MS spectra of the samples. Tandem mass spectrometry (MS^2) was performed to identify the radical species. The DMPO adducts with the C-centered radical species $[DMPO-R+H]^+$ are characterized by m/z 114 $[DMPO+H]^+$ in the MS^2 spectra and with peaks that represent the loss of $[DMPO+H]^+$. The DMPO adducts with O-centered radical species ($RO\cdot$ and $ROO\cdot$) are identified by m/z 130 $[DMPO-OH+H]^+$ and m/z 146 $[DMPO-O-OH+H]^+$, respectively, and with peaks that correspond to the loss of those adducts. DMPO was also able to capture OH radicals from the particle phase, and the product ion fragmentation confirmed DMPO/OH structure providing evidence for particle-bound OH radicals.

1 Introduction

Reactive oxygen species (ROS) present in the atmosphere include molecules such as hydrogen peroxide (H_2O_2), organic peroxides (ROOR) and hydroperoxides (ROOH), radical species like hydroxyl ($HO\cdot$), hydroperoxyl ($HOO\cdot$), peroxy ($ROO\cdot$) and alkoxy

Technical Note

J. Pavlovic and
P. K. Hopke

Title Page

Abstract

Introduction

Conclusions

References

Tables

Figures

◀

▶

◀

▶

Back

Close

Full Screen / Esc

Printer-friendly Version

Interactive Discussion

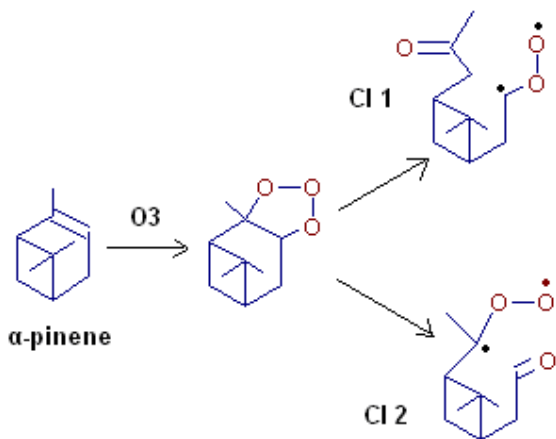


(RO·) radicals and ions like hypochlorite (OCl^-) and superoxide (O_2^-) ions. The hydroxyl radical ($\text{HO}\cdot$) is the most reactive oxidant in the troposphere (Seinfeld and Pandis, 2005). In the upper troposphere, it is formed in the reaction of a singlet oxygen $\text{O}(^1\text{D})$ and a water molecule:



The $\text{HO}\cdot$ radicals present in the lower troposphere (surface HO radical) come from the photolysis of ozone, photolysis of hydrogen peroxide or nitrous acid, Criegee intermediates (CI) decomposition, etc. These intermediates are formed by the reaction of ozone (O_3) and unsaturated compounds (alkenes) (Calvert et al., 2000).

10 One of the most intensively studied reactions under laboratory conditions is the reaction of O_3 with α -pinene ($\text{C}_{10}\text{H}_{16}$ monoterpene with an endocyclic double bond). The detailed mechanism of that reaction is described by Winterhalter et al. (2003) and Docherty et al. (2005). The two possible CI biradicals formed in that reaction are shown in Reaction (R2):



(R2)

Technical Note

J. Pavlovic and
P. K. Hopke

Title Page

Abstract

Introduction

Conclusions

References

Tables

Figures

◀

▶

◀

▶

Back

Close

Full Screen / Esc

Printer-friendly Version

Interactive Discussion



Technical Note

J. Pavlovic and
P. K. Hopke

Title Page

Abstract

Introduction

Conclusions

References

Tables

Figures

◀

▶

◀

▶

Back

Close

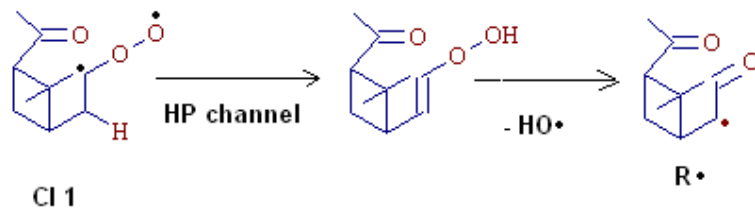
Full Screen / Esc

Printer-friendly Version

Interactive Discussion



Both intermediate products can be stabilized in reaction with water molecules or oxygenated organics (“stabilized Criegee intermediate SCI channel”) to form α -hydroxyhydroperoxides. Final products formed from that channel are carbonyls and acids. The CIs can also experience β -hydrogen migration to form HO \cdot radicals and alkyl radicals (R \cdot) through the “hydroperoxide channel” (Reaction R3).



(R3)

The alkyl radical (R \cdot) then reacts with oxygen to form an alkyl-peroxy radical (RO $_2\cdot$) that reacts with NO, HO $_2$, RO $_2$ and NO $_3$ to form alkoxy (RO \cdot) radicals leading to final oxidation products such as: hydroperoxides, alcohols, carbonyls, etc. (Kroll and Seinfeld, 2008).

Most of the first generation monoterpene oxidation products from α -pinene/ozone reactions have been identified (Winterhalter et al., 2003; Warscheid and Hoffmann, 2001). Recent work confirmed formation of dimer and higher molecular weight oligomers from the same reaction (Venkatachari and Hopke, 2008a; Gao et al., 2004). The mechanism of the polymerization processes involved in the oligomer formation is still unclear.

Recent studies have shown that significant amount of ROS is associated with ambient particulate matter (Venkatachari and Hopke, 2005) as well as with SOA formed under laboratory conditions during α -pinene/ozone reactions (Venkatachari and Hopke, 2008b). Hasson and Paulson (2003) measured gas- and aerosol-phase hydroperoxides present in urban air (West Los Angeles). Hydrogen peroxide was found to be the major hydroperoxide present and its aerosol mass loadings were found to be significantly higher than levels predicted by solubility of gaseous H $_2$ O $_2$ in water. However,

to date, there have been no studies performed to analyze and identify reactive radical species, other than HO· and HOO· radicals, formed either from monoterpene/ozone reactions or under ambient conditions in the gas phase.

Those reactive compounds can be involved in formation of first stage oxidation products (monomers) as well as higher molecular weight species (oligomers). Their role cannot stay underestimated over the other already characterized compounds. In vivo and in vitro toxicological and clinical studies have shown harmful health effects from endogenously formed ROS (Li et al., 2003; Harman, 1981; Dreher and Junod, 1996). The presence of ROS species in the water-soluble fraction of ultrafine and fine particles may be especially important because that fraction can carry toxics through the blood stream and cause adverse health effects. The redox active components present in particles are either ROS by its chemical composition or can induce ROS production in various cells in the lungs, blood and vascular tissues. The ROS can cause oxidative stress that results in damage of cellular membranes, DNA and proteins, and may exacerbate many inflammatory effects, such as asthma, chronic bronchitis, heart attacks, stroke, etc. (Delfino et al., 2005).

To determine the chemical composition of reactive oxygen and radical species, a spin trap was employed to stabilize the radicals and reduce their reactivity. Spin traps are diamagnetic compounds with double bonds that react with free radicals to form longer-lived radicals (the spin trap adducts) capable of being detected. The spin trap method is one of the most commonly employed methods for radical species detection and identification in organic and biological chemistry (Dominiques et al., 2003; Reis et al., 2003). Nitrones are the most frequently used spin traps, and spin trap adducts formed in their case are called nitroxides. Dubtsov et al. (2006) used α -phenyl nitron (PN); 1,2,2,5,5-pentamethyl-3-imidazoline-3-oxide (PMIO); and 3-hydroxyl-2-3-dihydro-2,2,5-trimethylpyrazine-1,4-dioxide (HDPDO) spin traps to identify short-lived gas-phase free radicals accompanying benzaldehyde photolysis. The same study used electron-spin-resonance spectroscopy (ESR) to record the spectra of the spin adducts. DMPO (5,5-dimethyl-4,5-dihydro-3H-pyrrole-N-oxide) was used by Shi et al. (2003) to

Technical Note

J. Pavlovic and
P. K. Hopke

[Title Page](#)[Abstract](#)[Introduction](#)[Conclusions](#)[References](#)[Tables](#)[Figures](#)[◀](#)[▶](#)[◀](#)[▶](#)[Back](#)[Close](#)[Full Screen / Esc](#)[Printer-friendly Version](#)[Interactive Discussion](#)

Technical NoteJ. Pavlovic and
P. K. Hopke

characterize hydroxyl radical production in collected filters of different size fractions of particulate matter (PM) to which H_2O_2 has been added. DMPO is one of the most commonly employed spin traps and is used in the present study. DMPO can trap both carbon-centered radicals and oxygen-centered radicals (Guo et al., 2003). The structure of DMPO is presented in Fig. 1 together with structures of its hydroxyl and hydroperoxyl adducts. Mass spectrometry (MS) was used for the detection and identification of the resulting spin trap adducts.

2 Experimental procedures

The reaction of α -pinene and O_3 was performed in the dark in a Pyrex flow reactor (Venkatachari and Hopke, 2008b). The length of the reactor was 120 cm (90 mm I.D.) and the volume 7.7 L. The residence time of the reactants in the chamber was 3.85 min. No $\text{HO}\cdot$ scavengers were used. Monoterpene vapor was produced by passing ultra high purity (99.999%) nitrogen through a midget impinger (25 ml) filled with α -pinene liquid (98% purity, Sigma Aldrich, USA). The vapor was then introduced into the reactor with a flow rate of 0.5 LPM. The resulting concentration of α -pinene was relatively constant between 2.5 to 3.0 ppmv for all of the experiments. The concentration of α -pinene entering the reactor was measured using gas chromatography-flame ionization detection (GC-FID; Thermo Finnigan, USA). Ozone was generated using an “Ozone Purification” system (Air Zone, VA, USA). The ozone was introduced into the reactor with a flow rate of 1.5 LPM with the resulting concentration of about 2.5 to 3.0 ppmv. Room air was used for the ozone generator after it passed through a high-efficiency particulate (HEPA) filter to remove any particulate matter. Unreacted ozone exiting the system was removed with a charcoal diffusion denuder. The α -pinene oxidation products exiting the denuder were collected at a 2 LPM final flow rate.

Particulate matter samples were collected for 30 min on 25 mm pre-baked quartz fiber filters (16 h at 550°C). The filters were immediately immersed into 10 ml of HPLC water that contained 0.5 mg of the DMPO spin trap (Alexis Biochemicals, Switzerland)

[Title Page](#)[Abstract](#)[Introduction](#)[Conclusions](#)[References](#)[Tables](#)[Figures](#)[◀](#)[▶](#)[◀](#)[▶](#)[Back](#)[Close](#)[Full Screen / Esc](#)[Printer-friendly Version](#)[Interactive Discussion](#)

Technical Note

J. Pavlovic and
P. K. Hopke

Title Page

Abstract

Introduction

Conclusions

References

Tables

Figures

◀

▶

◀

▶

Back

Close

Full Screen / Esc

Printer-friendly Version

Interactive Discussion



and then sonicated for 10 min. Because of the air- and light-sensitivity of the reagents, all reactions were conducted in the dark and under ultrahigh purity argon in an glove bag. The filter extracts were filtered through 0.45 μm AcrodiscTM syringe filters (Pall Gelman). The resulting samples were then analyzed using a Thermo Finnigan LCQ
5 Advantage ESI/MSⁿ system with direct sample injection without column separation. The ESI was employed in the positive (+) scan mode and the mass spectra were recorded over the mass range of m/z 100–1000. For MSⁿ experiments, the applied collision energies were between 30 and 35% (100% collision energy corresponds to 5 V) using helium as the collision gas. Ten (10) samples were collected and analyzed
10 for the same reaction and laboratory conditions. As a negative control (blank), a mixture of HPLC water and DMPO solution with a pre-baked quartz fiber filter was sonicated for 10 min, filtered and analyzed under the same instrumental conditions.

3 Results and discussion

3.1 Full MS spectrum m/z 100–1000 (sample vs. blank)

15 In order to identify the DMPO-free radical adducts produced by the α -pinene /ozone reaction, the full mass spectra of the samples and blanks were compared as in Fig. 2. In both spectra, ions with m/z 114 and m/z 227 were observed and correspond to the quasi-molecular ion $[\text{DMPO}+\text{H}]^+$ and molecular cluster $[\text{2DMPO}+\text{H}]^+$, respectively. After the monoterpene oxidation (sample+DMPO), new ions were observed indicating
20 a new species had been formed. In the low mass region (m/z 100– m/z 250), positive ions with m/z 130 had the highest intensity compared with m/z 114. Other ions found in that region are expected to be α -pinene oxidation products containing keto, aldehyde, hydroxyl and epoxy functional groups. Those groups have a sufficient proton affinity to appear as positive quasi-molecular ions $[\text{M}+\text{H}]^+$ in the ESI (+) scan mode, and have
25 been identified and discussed in more detail by Winterhalter et al. (2003) and Glasius et al. (1999).

Technical Note

J. Pavlovic and
P. K. Hopke

Title Page

Abstract

Introduction

Conclusions

References

Tables

Figures

◀

▶

◀

▶

Back

Close

Full Screen / Esc

Printer-friendly Version

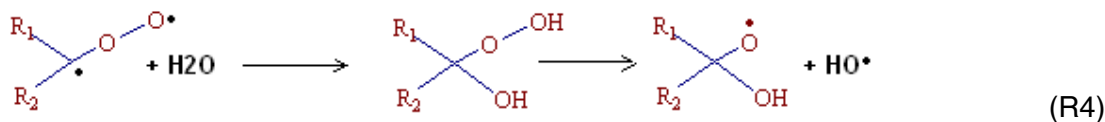
Interactive Discussion

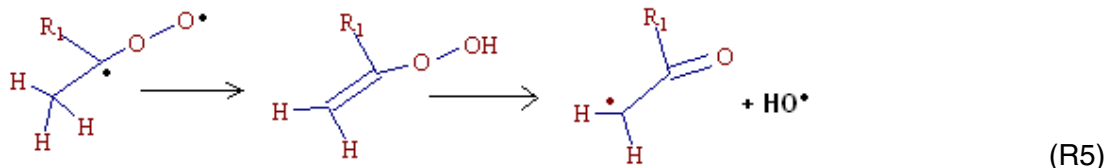


In the higher mass range ($m/z > 250$), clusters were observed separated by 12–16 amu (Fig. 2). Adjacent ions in the single clusters were separated by 1 amu, indicating that only single charged ions were present. Similar patterns in the ESI-QTOF mass spectrum were found by Tolocka et al. (2004) for SOA produced by reaction of α -pinene and ozone without a spin trap agent. In the present work, peaks into clusters represent possible DMPO adducts with reactive radical species formed from α -pinene/ozone reactions.

3.2 MS² fragmentation results

Figure 3 shows the MS² spectrum of the DMPO-free radical adducts with an m/z 130. The same figure also illustrates possible structure of that adduct and structures of its fragments. The fragmentation patterns indicate that a DMPO adduct was formed with the hydroxyl (HO·) radical and a similar spectrum was shown by Yang et al. (2007). The relatively high intensity of the peak with m/z 130 compared to the other peaks supports the role of the “hydroperoxide channel” as an important pathway in monoterpene ozonolysis. Winterhalter et al. (2003) reported that 77% of oxidation products are formed through this channel. Aschmann et al. (2002) measured the HO yield from α -pinene/ozone reactions to be 0.77 ± 0.10 . Anglada et al. (2002) suggested that α -hydroxyhydroperoxides formed through the SCI channel can also be an important source of HO radicals. The peroxide bond can undergo O–O cleavage because of the excess in internal energy and form HO· and alkoxy RO· (Reaction R4) or alkyl R· radicals (Reaction R5).





The positive ion with m/z 146 (or m/z 147–148) that would be assigned to the DMPO adduct with HO_2 radicals was not observed in the full mass spectrum. This result could be due to the very fast conversion of HO_2 radicals to HO radicals via:



or the formation of a hydrogen peroxide molecule:



Another possibility could be the spontaneous transformation of DMPO/OOH adducts to DMPO/OH adducts (Bacic et al., 2008), which is one of the major disadvantages of DMPO in spin trap applications.

Table 1 presents the fragment ions observed in the MS/MS spectra of the most abundant DMPO adducts. Major signals in MS^2 spectra belong to protonated forms of the spin trap $[\text{DMPO}+\text{H}]^+$ with m/z 114. Peaks with m/z 130, m/z 131 and m/z 132 correspond to protonated, oxidized, radical and reduced forms of $[\text{DMPO}-\text{OH}+\text{H}]^+$ adducts (Fig. 4a). The MS^2 fragmentation of a few spin trap adducts (m/z 314, m/z 371 and m/z 452) revealed the peaks with m/z 146, m/z 147 and m/z 148. Those ions can be assigned to protonated, oxidized, radical and reduced forms of $[\text{DMPO}-\text{OOH}+\text{H}]^+$ adducts (Fig. 4b). The other major fragment ions present in MS^2 spectra were losses of: $[\text{DMPO}]$, $[\text{DMPO}+\text{H}]^+$, $[\text{DMPO}-\text{OH}+\text{H}]^+$, $[\text{DMPO}-\text{OOH}+\text{H}]^+$ and loss of water molecules.

Technical Note

J. Pavlovic and
P. K. Hopke

Title Page

Abstract

Introduction

Conclusions

References

Tables

Figures

◀

▶

◀

▶

Back

Close

Full Screen / Esc

Printer-friendly Version

Interactive Discussion



3.3 Carbon-centered radical species

Some of the observed spin trap adducts (m/z 268, m/z 324 and m/z 439) only contain peaks with m/z 114 $[\text{DMPO}+\text{H}]^+$ in their MS^2 spectra, in addition to peaks that represent the loss of $[\text{DMPO}]$, $[\text{DMPO}+\text{H}]^+$ and water molecules. Those adducts can be a result of the reaction of the DMPO and C-centered radical species ($\text{R}\cdot$). One example is the adduct with m/z 268, whose MS^2 spectrum is presented in Fig. 5. The most abundant ion in that spectrum is m/z 154 that can be assigned to a protonated form of the radical specie $[\text{R}\cdot+\text{H}]^+$ and corresponds to the loss of $[\text{DMPO}+\text{H}]^+$ with m/z 114. Other positive ions found in the spectrum are $[\text{DMPO}+\text{H}]^+$ with m/z 114 and peaks that represent loss of a water molecule and loss of m/z 57 (possibly deprotonated acetone). The fragment ion with m/z 57 was observed in MS^2 spectrums (ESI in negative mode) of many monoterpene/ozone reaction products reported by Warscheid and Hoffmann (2001). Carbon-centered radical species are not considered to be reactive oxygen species, but further reactions in the presence of oxygen can lead to $\text{RO}_2\cdot$ and $\text{RO}\cdot$ formation.

3.4 Oxygen-centered radical species

Spin trap adducts with m/z 314, m/z 371 and m/z 452 have in their MS^2 spectra peaks with m/z 131 and m/z 146 in addition to the m/z 114. Those adducts can be formed in a reaction of the DMPO and O-centered radical species, in this case, peroxy radicals ($\text{ROO}\cdot$). The example presented in Fig. 6 has m/z 314 and a possible structure of $[\text{DMPO}-\text{O}-\text{O}-\text{R}+\text{H}]^+$. The ion with m/z 131 can be assigned to a protonated radical form of $[\text{DMPO}-\text{OH}+\text{H}]^+$ and the ion with m/z 146 could be the protonated oxidized form of $[\text{DMPO}-\text{O}-\text{OH}+\text{H}]^+$. The ion with m/z 146 could be evidence that the captured radical had the peroxy ($\text{ROO}\cdot$) structure and the formed adduct had the $[\text{DMPO}-\text{O}-\text{O}-\text{R}+\text{H}]^+$ structure. During the process of MS^2 fragmentation, one of the weakest bonds in that structure, the O-R bond, suffers cleavage, resulting in a peak with m/z 146. The strongest product signals in the same spectrum correspond to the

Technical Note

J. Pavlovic and
P. K. Hopke

[Title Page](#)[Abstract](#)[Introduction](#)[Conclusions](#)[References](#)[Tables](#)[Figures](#)[◀](#)[▶](#)[◀](#)[▶](#)[Back](#)[Close](#)[Full Screen / Esc](#)[Printer-friendly Version](#)[Interactive Discussion](#)

loss of a H₂O molecule (–18Da) and the loss of deprotonated acetone (–57Da). Reis et al. (2003) found the same fragment ions with *m/z* 146 from linoleic acid oxidation and assigned that fragment ions to [DMPO–O–OH+H]⁺ adducts.

All the other spin trap adducts tabulated in Table 1 had present, in their MS² spectra, peaks with *m/z* 114, *m/z* 130, and also peaks that correspond to the losses of: [DMPO], [DMPO+H]⁺, [DMPO–OH+H]⁺ and water molecules. Those peaks can be assigned to the adducts of the alkoxy (RO·) radicals with DMPO. The example presented in Fig. 7 had an *m/z* 299 and a possible structure of [DMPO–O–R+H]⁺. The most abundant ion with *m/z* 114 corresponds to the [DMPO+H]⁺ adduct and the ion with *m/z* 185 corresponds to the loss of that adduct. The ion with *m/z* 130 could be the protonated, oxidized form of the [DMPO–OH+H]⁺ adduct, with *m/z* 169 representing the loss of that adduct.

The alkoxy radical identification is supported by Guo et al. (2003). That study also showed the presence of [DMPO–OH+H]⁺ ions with *m/z* 131 in MS² spectra of the DMPO/alkoxy radical adducts formed with *t*-butyl and cumene hydroperoxide. Furthermore, major fragment ions found in the MS³ spectrum of the ion with *m/z* 131 were the same as those found in the MS² spectrum of the synthesized DMPO/hydroxyl radical adduct and the same as ions found in the present study from fragmentation of the ion with *m/z* 130 (Fig. 3). Therefore, it is reasonable to believe that adducts that contain *m/z* 130 (and not *m/z* 146) in their MS² spectra are formed from DMPO and alkoxy radicals.

A large number of [DMPO–O–R+H]⁺ adducts and only few [DMPO–O–OR+H]⁺ adducts can be due to the DMPO/OOH spontaneous transformation and also due to the fast self-reaction of RO₂ radicals under NO_x-free conditions to form RO radicals (Reaction R8).



The reaction mechanisms suggested by Anglada et al. (2002) also support the formation of a large number of alkoxy radical adducts. Those adducts may not

Technical Note

J. Pavlovic and
P. K. Hopke

[Title Page](#)[Abstract](#)[Introduction](#)[Conclusions](#)[References](#)[Tables](#)[Figures](#)[◀](#)[▶](#)[◀](#)[▶](#)[Back](#)[Close](#)[Full Screen / Esc](#)[Printer-friendly Version](#)[Interactive Discussion](#)

always come from the “hydroperoxide channel.” The O–O bond cleavage in α -hydroxyhydroperoxides results in HO· and RO· formation and subsequent DMPO/OH and DMPO/OR adducts.

4 Conclusions

5 In summary, this study took the novel approach of using a spin trap to capture and MS² to characterize radical species from a monoterpene/ozone reaction. The method is quick and has the potential to be applied to rapid screening of radical species present in the airborne particulate matter samples. Furthermore, this study provided evidence of the presence of OH radicals in the particulate phase from the monoterpene/ozone
10 reaction. It is still unclear whether the OH radicals are formed during condensation processes directly from the reaction chamber or they are generated afterwards by reactions on filters during the collection interval. The short residence time (3.85 min) supports the fact that OH radicals are formed during the collection, but it does not diminish its potential for adverse health effects. In either case, OH radicals can upset the
15 redox balance within the cells and cause oxidative stress.

The nitron spin trap (DMPO) was successful in the trapping of C-centered radicals (R·) as well as two types of O-centered radicals (RO· and ROO·). DMPO/OOR adducts can suffer spontaneous transformation to form DMPO/OR adducts. At this point, it is impossible to say with certainty which adducts (DMPO/OR or DMPO/OOR) are formed
20 first. Detailed structures of radical species captured in this study are still unknown and require further investigation.

Acknowledgements. This work was supported by US Environmental Protection Agency's Science to Achieve Results (STAR) Program through a subcontract from the University of Rochester PM and Health Center Grant RD832415. Although the research described in this
25 article has been funded wholly or in part by the United States Environmental Protection Agency, it has not been subjected to the Agency's required peer and policy review and therefore, does not necessarily reflect the views of the Agency and no official endorsement should be inferred.

Technical Note

J. Pavlovic and
P. K. Hopke

Title Page

Abstract

Introduction

Conclusions

References

Tables

Figures

◀

▶

◀

▶

Back

Close

Full Screen / Esc

Printer-friendly Version

Interactive Discussion



References

- Anglada, J. M., Aplincourt, P., Bofill, J. M., and Cremer, D.: Atmospheric formation of OH radicals and H₂O₂ from alkene ozonolysis under humid conditions, *Chem. Phys. Chem.*, 3, 215–221, 2002.
- 5 Aschmann, S. M., Arey, J., and Atkinson, R.: OH radical formation from the gas-phase reactions of O₃ with a series of terpenes, *Atmos. Environ.*, 36, 4347–4355, 2002.
- Bacic, G., Spasojevic, I., Secerov, B., and Mojovic, M.: Spin-trapping of oxygen free radicals in chemical and biological systems: new traps, radicals and possibilities, *Spectrochim. Acta A*, 69, 1354–1366, 2008.
- 10 Calvert, J. G., Atkinson, R., Keer, J. A., Madronich, S., Moortgat, G. K., Wallington, T. J., and Yarwood, G.: *The Mechanisms of Atmospheric Oxidation of the Alkenes*, Oxford University Press, New York, 2000.
- Delfino, R. J., Sioutas, S., and Malik, S.: Potential role of ultrafine particles in associations between airborne particle mass and cardiovascular health, *Environ. Health Persp.*, 113, 934–946, 2005.
- 15 Docherty, K. S., Wu, W., Lim, Y. B., and Ziemann, P. J.: Contributions of organic peroxides to secondary organic aerosol formed from reactions of monoterpenes with O₃, *Environ. Sci. Technol.*, 39, 4049–4059, 2005.
- Dominques, M. R. M., Dominques, P., Reis, A., Fonseca, C., Amado, F. M. L., and Ferrer-Correia, A. J. V.: Identification of oxidation products and free radicals of tryptophan by mass spectrometry, *Am. Soc. Mass Spectr.*, 14, 406–416, 2003.
- 20 Dreher, D. and Junod, A. F.: Role of oxygen free radicals in cancer development, *Eur. J. Cancer*, 32A, 30–38, 1996.
- Dubtsov, S. N., Dultseva, G. G., Dultsev, E. N., and Skubnevskaya, G. I.: Investigation of aerosol formation during benzaldehyde photolysis, *J. Phys. Chem. B*, 110, 645–649, 2006.
- 25 Gao, S., Ng, N. L., Keywood, M., Varutbangkul, V., Bahreini, R., Nenes, A., He, J., Yoo, K. Y., Beauchamp, J. L., Hodyss, R. P., Flagan, R. C., and Seinfeld, J. H.: Particle phase acidity and oligomer formation in secondary organic aerosol, *Environ. Sci. Technol.*, 38, 6582–6589, 2004.
- 30 Glasius, M., Duane, M., and Larsen, B. R.: Analysis of polar terpene oxidation products in aerosols by liquid chromatography ion trap mass spectrometry (MSⁿ), *J. Chromatogr.*, 833, 121–135, 1999.

Technical Note

J. Pavlovic and
P. K. Hopke

Title Page

Abstract

Introduction

Conclusions

References

Tables

Figures

◀

▶

◀

▶

Back

Close

Full Screen / Esc

Printer-friendly Version

Interactive Discussion



Technical Note

J. Pavlovic and
P. K. Hopke

Title Page

Abstract

Introduction

Conclusions

References

Tables

Figures

◀

▶

◀

▶

Back

Close

Full Screen / Esc

Printer-friendly Version

Interactive Discussion



Guo, Q., Qian, S. Y., and Mason, R. P.: Separation and identification of DMPO adducts of oxygen-centered radicals formed from organic hydroperoxides by HPLC-ESR, ESI-MS and MS/MS, *Am. Soc. Mass Spectr.*, 14, 862–871, 2003.

Harman, D.: The aging process, *Proc. Natl. Acad. Sci. USA*, 78(11), 7124–7128, 1981.

Hasson, A. S. and Paulson, S. E.: An investigation of the relationship between gas-phase and aerosol-borne hydroperoxides in urban air, *J. Aerosol Sci.*, 34, 459–468, 2003.

Kroll, J. H. and Seinfeld, J. H.: Chemistry of secondary organic aerosol: formation and evolution of low-volatility organics in the atmosphere, *Atmos. Environ.*, 42, 3593–3624, 2008.

Li, N., Hao, M., Phalen, R. F., Hinds, W. C., and Nel, A. E.: Particulate air pollutants and asthma. A paradigm for the role of oxidative stress in PM-induced adverse health effects, *Clin. Immunol.*, 109, 250–265, 2003.

Reis, A., Dominques, M. R. M., Amado, F. M. L., Ferrer-Correia, A. J. V., and Dominques, P.: Detection and characterization by mass spectrometry of radical adducts produced by linoleic acid oxidation, *Am. Soc. Mass Spectr.*, 14, 1250–1261, 2003.

Seinfeld, J. H. and Pandis, S. N.: *Atmospheric Chemistry and Physics: From Air Pollution to Climate Change*, John Wiley and Sons, Inc., New Jersey, 2006.

Shi, T., Schins, R. P. F., Knaapen, A. M., Kuhlbusch, T., Pitz, M., Heinrich, J., and Borm, P. J. A.: Hydroxyl radical generation by electron paramagnetic resonance as a new method to monitor ambient particulate matter composition, *J. Environ. Monitor.*, 5, 550–556, 2003.

Tolocka, M. P., Jang, M., Ginter, J. M., Cox, F. J., Kamens, R. M., and Johnston, M. V.: Formation of oligomers in secondary organic aerosol, *Environ. Sci. Technol.*, 38, 1428–1434, 2004.

Venkatachari, P., Hopke, P. K., Grover, B. D., and Eatough, D. J.: Measurement of particle-bound reactive oxygen species in Rubidoux aerosols, *J. Atmos. Chem.*, 50, 49–58, 2005.

Venkatachari, P. and Hopke, P. K.: Characterization of products formed in the reaction of ozone with α -pinene: case for organic peroxides, *J. Environ. Monitor.*, 10, 966–974, 2008a.

Venkatachari, P. and Hopke, P. K.: Development and evaluation of a particle-bound reactive oxygen species generator, *J. Aerosol Sci.*, 39, 168–174, 2008b.

Warscheid, B. and Hoffmann, T.: Structural elucidation of monoterpene oxidation products by ion trap fragmentation using on-line atmospheric pressure chemical ionization mass spectrometry in the negative ion mode, *Rapid Commun. Mass Sp.*, 15, 2259–2272, 2001.

Winterhalter, R., Van Dingenen, R., Larsen, B. R., Jensen, N. R., and Hjorth, J.: LC-MS analysis of aerosol particles from the oxidation of α -pinene by ozone and OH-radicals, *Atmos. Chem. Phys. Discuss.*, 3, 1–39, 2003,

<http://www.atmos-chem-phys-discuss.net/3/1/2003/>.

Yang, F., Zhang, R., He, J., and Abliz, Z.: Development of a liquid chromatography/ electrospray ionization tandem mass spectrometric method for the determination of hydroxyl radical, Rapid Commun. Mass Sp., 21, 107–111, 2007.

ACPD

9, 23695–23717, 2009

Technical Note

J. Pavlovic and
P. K. Hopke

Title Page

Abstract

Introduction

Conclusions

References

Tables

Figures

◀

▶

◀

▶

Back

Close

Full Screen / Esc

Printer-friendly Version

Interactive Discussion



Technical Note

J. Pavlovic and
P. K. Hopke

Table 1. Fragment ions found in MS² spectra of the most abundant DMPO adducts.

DMPO adducts	Fragment ions							-H ₂ O
	[DMPO+H] ⁺	[DMPO-OH+H] ⁺	[DMPO-O-OH+H] ⁺	-[DMPO]	-[DMPO+H] ⁺	-[DMPO-OH+H] ⁺	-[DMPO-O-OH+H] ⁺	
<i>m/z</i> 268	+			+	+			+
<i>m/z</i> 284	+	+		+	+	+		+
<i>m/z</i> 299	+	+		+	+	+		+
<i>m/z</i> 314	+	+	+	+	+	+	+	+
<i>m/z</i> 324	+			+	+			+
<i>m/z</i> 340	+	+		+	+	+		+
<i>m/z</i> 356	+	+		+	+	+	+	+
<i>m/z</i> 371	+	+	+	+	+	+		+
<i>m/z</i> 409		+		+	+	+		+
<i>m/z</i> 425		+		+	+	+		+
<i>m/z</i> 439	+			+	+	+		+
<i>m/z</i> 452		+	+	+	+	+	+	+

+: fragment ion present in MS² spectra

[Title Page](#)
[Abstract](#)
[Introduction](#)
[Conclusions](#)
[References](#)
[Tables](#)
[Figures](#)
[Back](#)
[Close](#)
[Full Screen / Esc](#)
[Printer-friendly Version](#)
[Interactive Discussion](#)


Technical Note

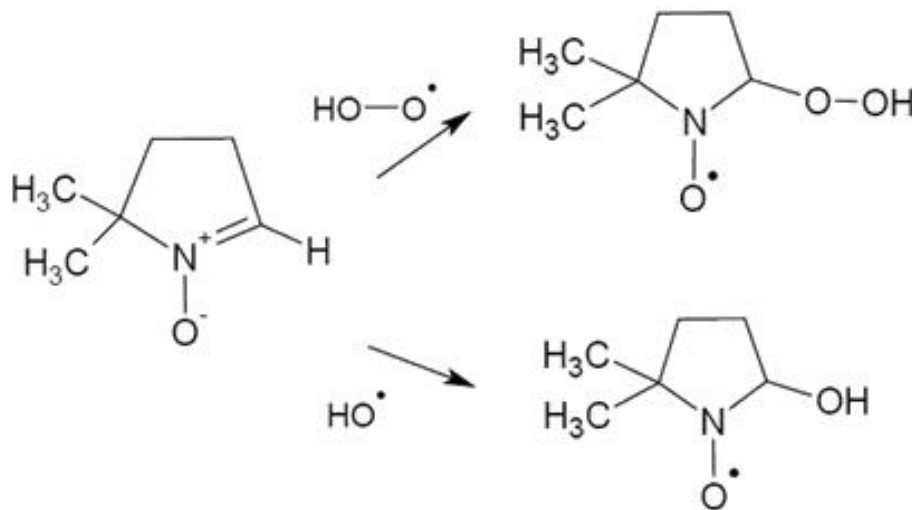
J. Pavlovic and
P. K. Hopke

Fig. 1. Structures of DMPO and its hydroxyl and hydroperoxyl adducts.

[Title Page](#)[Abstract](#)[Introduction](#)[Conclusions](#)[References](#)[Tables](#)[Figures](#)[◀](#)[▶](#)[◀](#)[▶](#)[Back](#)[Close](#)[Full Screen / Esc](#)[Printer-friendly Version](#)[Interactive Discussion](#)

Technical Note

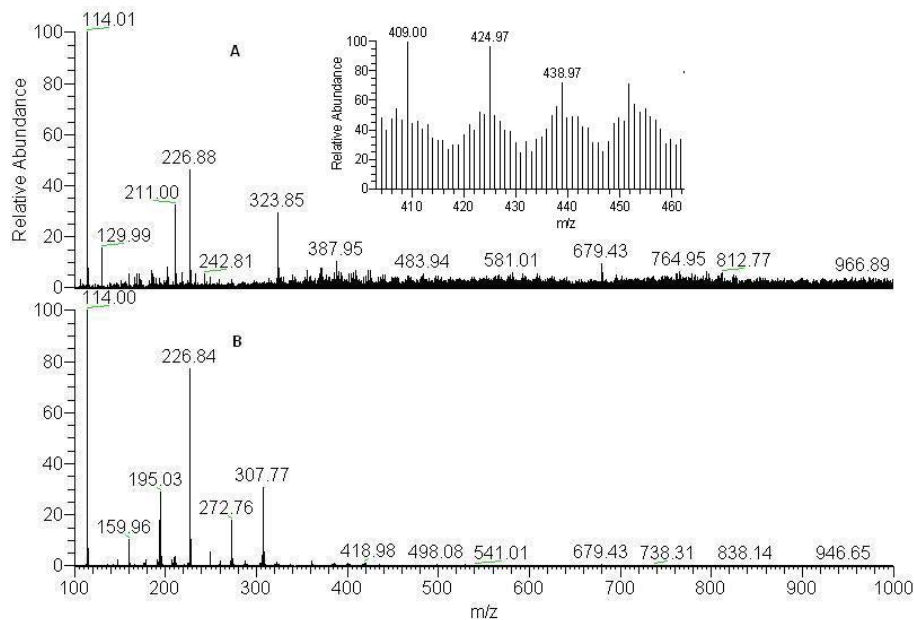
J. Pavlovic and
P. K. Hopke

Fig. 2. Full MS (m/z 100–1000) of sample (a) and blank (b).

[Title Page](#)[Abstract](#)[Introduction](#)[Conclusions](#)[References](#)[Tables](#)[Figures](#)[I◀](#)[▶I](#)[◀](#)[▶](#)[Back](#)[Close](#)[Full Screen / Esc](#)[Printer-friendly Version](#)[Interactive Discussion](#)

Technical Note

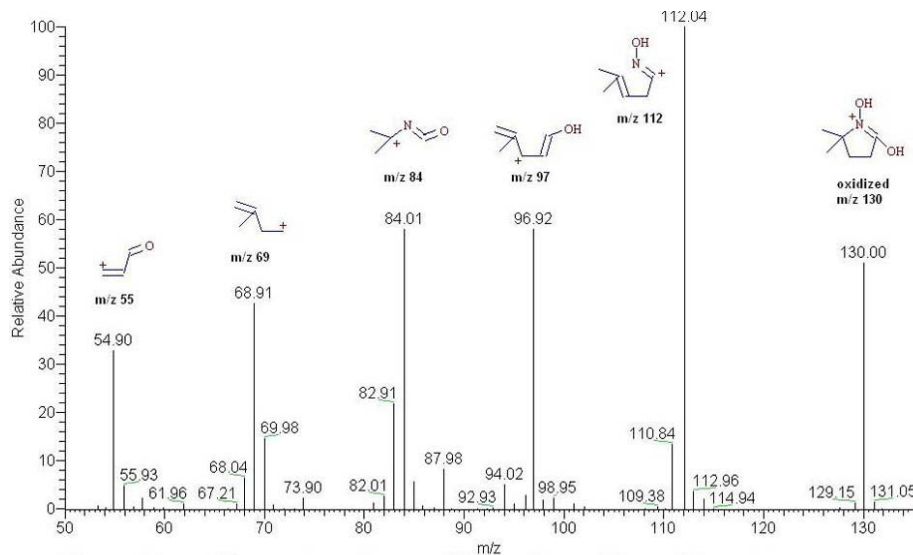
J. Pavlovic and
P. K. Hopke

Fig. 3. MS^2 fragmentation of the adduct with m/z 130 with possible structures of formed fragments.

[Title Page](#)[Abstract](#)[Introduction](#)[Conclusions](#)[References](#)[Tables](#)[Figures](#)[◀](#)[▶](#)[◀](#)[▶](#)[Back](#)[Close](#)[Full Screen / Esc](#)[Printer-friendly Version](#)[Interactive Discussion](#)

Technical Note

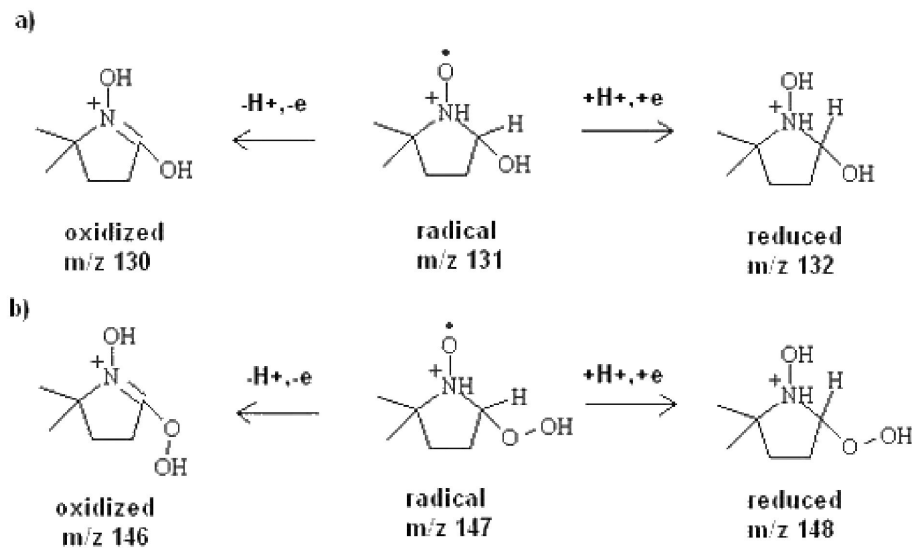
J. Pavlovic and
P. K. Hopke

Fig. 4. Protonated structures of the oxidized, radical and reduced forms of DMPO/OH (a) and DMPO/OOH (b) adducts.

[Title Page](#)[Abstract](#)[Introduction](#)[Conclusions](#)[References](#)[Tables](#)[Figures](#)[I◀](#)[▶I](#)[◀](#)[▶](#)[Back](#)[Close](#)[Full Screen / Esc](#)[Printer-friendly Version](#)[Interactive Discussion](#)

Technical Note

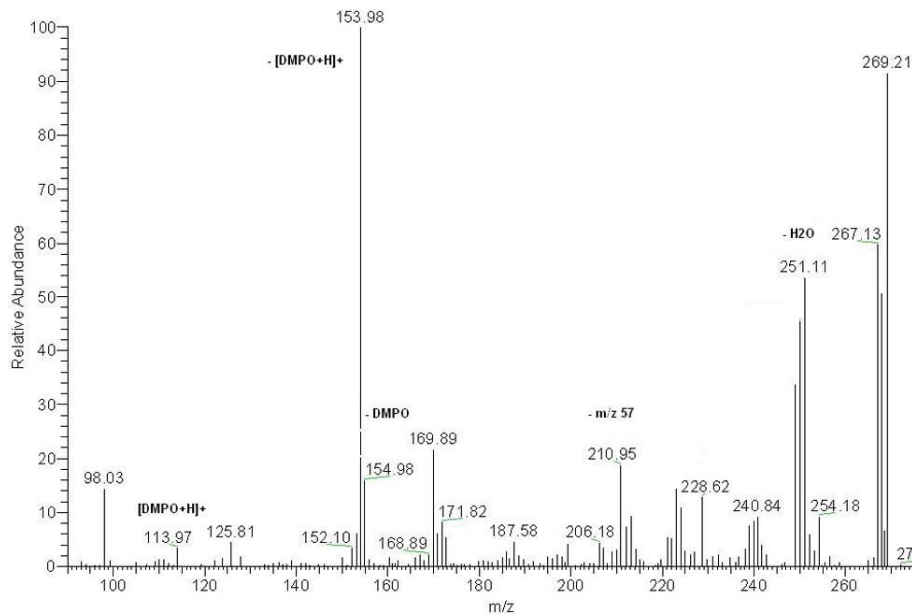
J. Pavlovic and
P. K. Hopke

Fig. 5. MS² spectrum of the adduct with m/z 268.

[Title Page](#)[Abstract](#)[Introduction](#)[Conclusions](#)[References](#)[Tables](#)[Figures](#)[◀](#)[▶](#)[◀](#)[▶](#)[Back](#)[Close](#)[Full Screen / Esc](#)[Printer-friendly Version](#)[Interactive Discussion](#)

Technical Note

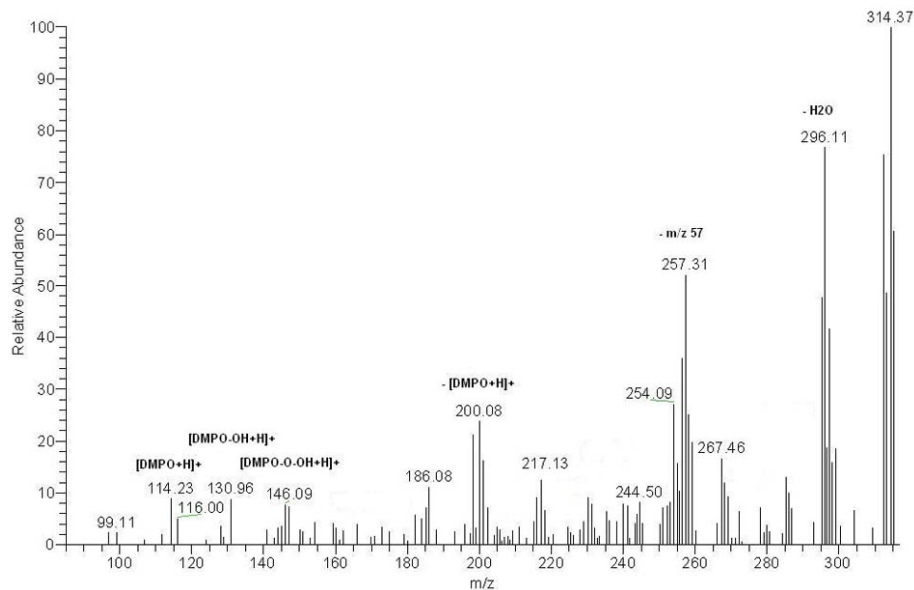
J. Pavlovic and
P. K. Hopke

Fig. 6. MS² spectrum of the adduct with m/z 314.

[Title Page](#)[Abstract](#)[Introduction](#)[Conclusions](#)[References](#)[Tables](#)[Figures](#)[◀](#)[▶](#)[◀](#)[▶](#)[Back](#)[Close](#)[Full Screen / Esc](#)[Printer-friendly Version](#)[Interactive Discussion](#)

Technical Note

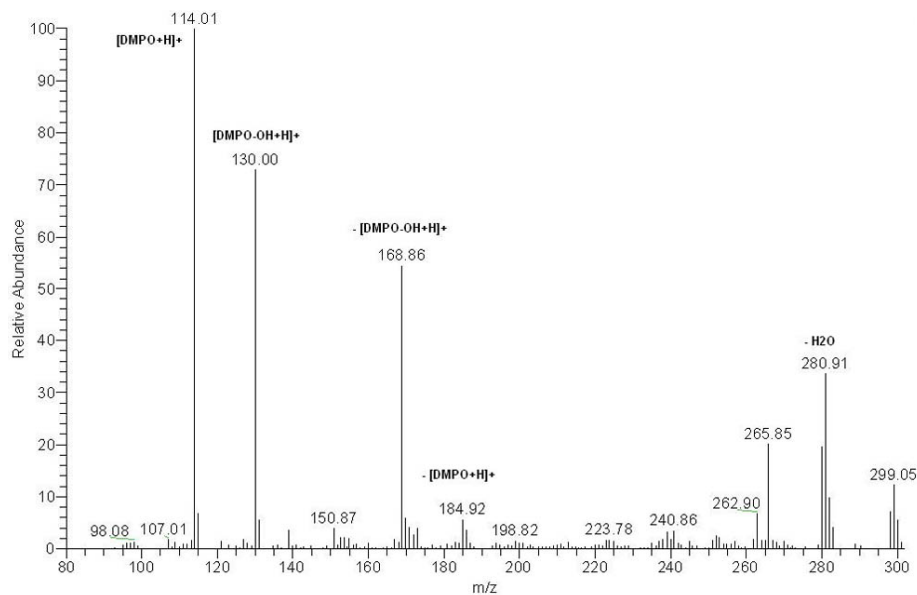
J. Pavlovic and
P. K. Hopke

Fig. 7. MS² spectrum of the adduct with m/z 299.

[Title Page](#)[Abstract](#)[Introduction](#)[Conclusions](#)[References](#)[Tables](#)[Figures](#)[◀](#)[▶](#)[◀](#)[▶](#)[Back](#)[Close](#)[Full Screen / Esc](#)[Printer-friendly Version](#)[Interactive Discussion](#)